



STABILITY ESTIMATES FOR DISCRETE DUALITY FINITE VOLUME SCHEME FOR HESTON MODEL*

ANGELA HANDLOVIČOVÁ

Slovak University of Technology, Bratislava Slovakia
angela.handlovicova@stuba.sk

Abstract

Tensor diffusion equation represents an important model in many field of science. We focused our attention to the problem which arises in financial mathematics and is known as 2D Heston model. Stability estimates for discrete duality finite volume scheme for Heston model is presented. Numerical experiments using proposed method and comparing it with previous numerical scheme are included.

Key words: Heston model, tensor diffusion, discrete duality finite volume method, numerical solution, stability estimates

1. INTRODUCTION

Mathematical model investigated in this paper comes from financial mathematics and represents generalization of Black and Scholes model for option pricing. First we briefly describe the historical background that caused the creation of Heston model. For more details see Kútik (2013) and references therein. Black and Scholes published their seminal paper (1973) on the theory of option pricing. Their formulation of the option pricing theory has soon become very attractive, since the final valuation formulas deduced from their model is a function of only a few observable variables (except the volatility parameter). Because of its simplicity, the accuracy of the model can be proved quite straight-forward by direct empirical tests with market data and the price of an option in an idealized financial market can be computed from a solution to a linear parabolic equation. A further research of the basic linear Black-Scholes framework has led to generalized and more realistic

models. Many of those generalizations transform the classical linear parabolic differential equation into a non-linear one where the volatility parameter is no longer a constant but a general function dependent from the second derivative of the option price.

Historically, most market practitioners had not demanded any major changes or other upgrades of the classical Black-Scholes model until the big market crash in 1987. After this breakdown the skepticism regarding the Black-Scholes underlying assumptions as well as the need for incorporation of stochastic volatility into the models have become evident. Academic community as well as practitioners realized the vast possibilities of such an approach and since then many other stochastic volatility models have been proposed. Nowadays, one of the most commonly used is the one introduced by Heston (1993).

The Heston model is interesting from mathematical point of view too, because it can be represent by a parabolic two dimensional tensor diffusion equa-

* This work was supported by grants VEGA 1/0728/15 and APVV-15-0522

tion with degenerate tensor on the part of the boundary, where so called Fichera condition is fulfilled. For this model, numerical scheme based on finite volume method is presented in Kútík and Mikula (2015), where several numerical experiments using this scheme are presented. From numerical analysis point of view, the existence and uniqueness of a numerical solution is proved.

Recently we present so called discrete duality finite volume method (DDFV) for Heston model in Handlovičová (2016), where similar theoretical results are obtained and numerical experiments show better behaviour of numerical solution obtain by DDFV scheme for Heston model as for classical finite volume case. That is why we further investigate this task and here we present stability estimates for the proposed scheme.

2. HESTON MODEL

Heston model in transformed form can be represented by

$$\frac{\partial v}{\partial \tau} + \vec{A} \cdot \nabla v = \nabla \cdot (B \nabla v) - rv, \text{ in } \Omega \times [t_1, t_2], \quad (1)$$

where unknown function is $v = v(x, y, \tau)$ and

$$B = \frac{1}{2}y \begin{pmatrix} 1 & \rho\sigma \\ \rho\sigma & \sigma^2 \end{pmatrix}, \quad (2)$$

$$\vec{A} = - \begin{pmatrix} r - \frac{1}{2}y - \frac{1}{2}\rho\sigma \\ \kappa(\theta - y) - \lambda y - \frac{1}{2}\sigma^2 \end{pmatrix}.$$

Ω is rectangular 2D domain $\Omega = (X_a, X_b) \times (0, Y)$ and $[t_1, t_2]$ is time interval: $0 < t_1 < t_2 < \infty$.

In original Heston model unknown function $V(S, \nu, t)$ represents the value of option price for stock price S and variance of underlying asset ν in time to the maturity t . In transformed model (1) we use new variables $(x, y, \tau) = (\ln(S), \nu, T - t)$ where T is an expiration time. The financial parameters of the model are (see Kútík, 2013): ρ - correlation parameter, κ - reversion speed, σ - the volatility variance, θ - long term variance, r - interest rate. They have the following properties: $\rho \in \langle -1, 1 \rangle$, $\sigma > 0$, $r > 0$, $\kappa > 0$, $\theta > 0$, $\lambda > 0$.

The above problem can be endowed with the initial condition and boundary conditions of the type

$$v(x, y, 0) = \max(0, e^x - 1),$$

$$v(X_a, y, \tau) = 0,$$

$$v(X_b, y, \tau) = e^{X_b} - e^{-r\tau}, \quad (3)$$

$$\frac{\partial v(x, Y, \tau)}{\partial \mathbf{n}} = 0,$$

where \mathbf{n} is the outward normal to the boundary $\partial\Omega$. For the boundary $y = 0$ no boundary condition must be prescribed because it is a consequence of so called Fichera condition and we used the similar treatment as is prescribed in Kútík and Mikula (2015). In our situation this condition can be expressed in the form

$$\kappa\theta - \frac{1}{2}\sigma^2 \geq 0. \quad (4)$$

To obtain stability estimates we will find the function $v = v(x, y, \tau)$ in the form $v(x, y, \tau) = u(x, y, \tau) + w(x, y, \tau)$, where function w is of the form

$$w(x, y, \tau) = \frac{x - X_a}{X_b - X_a} (e^{X_b} - e^{-r\tau}) \quad (5)$$

and fulfils prescribed initial and boundary conditions (3).

For function u the following problem holds:

$$\frac{\partial u}{\partial \tau} + \vec{A} \cdot \nabla u = \nabla \cdot (B \nabla u) - ru + f(x, y, \tau),$$

$$\text{in } \Omega \times [t_1, t_2], \quad (6)$$

where

$$f(x, y, \tau) = -\frac{1}{X_b - X_a} \left(r(x - X_a)e^{X_b} - \frac{y}{2}(e^{X_b} - e^{-r\tau}) - \left(\frac{\rho\sigma}{2} - r\right)(e^{X_b} - e^{-r\tau}) \right)$$

and function u fulfils homogeneous initial and boundary conditions.

3. DISCRETIZATION

We present here fully implicit scheme. For discretization in time we use uniform discrete time step $k = \frac{t_2 - t_1}{N}$ and $t_n = nk$ for $n = 0, 1, \dots, N$. The time derivative is approximated using the backward difference. We denote by u^n the piecewise constant function on each time interval $[t_{n-1}, t_n]$, $n = 1, \dots, N$. Further we denote by f^n the average value of a function f on each time interval $[t_{n-1}, t_n]$ and similarly it is the piecewise constant function on each time interval $[t_{n-1}, t_n]$. We have

$$\frac{u^n - u^{n-1}}{k} = \nabla \cdot (B \nabla u^n) - \nabla \cdot (\vec{A} u^n) + (\nabla \cdot \vec{A}) u^n - ru^n + f^n. \quad (7)$$

For the space discretization we use method based on finite volumes. That means our numerical solution will be piecewise constant function on each finite volume V_{ij} and each time interval $[t_{n-1}, t_n]$. We denote it by u_{ij}^n and similarly we denote by f_{ij}^n



the piecewise constant function on each finite volume V_{ij} and each time interval $[t_{n-1}, t_n]$ as an average function on each finite volume and time interval. For the sake of simplicity we will use the notation: $x := (x, y) \in \Omega$. Moreover in financial mathematics (Heston model) and in image processing problems (anisotropic tensor diffusion model) we often use the rectangular domain in 2D. Following Handlovičová (2016) our finite volume mesh will consist of cells $V_{ij} \in \mathcal{T}_h$ with the measure $m(V_{ij})$, associated with DF nodes $x_{ij} := (x_{ij}, y_{ij}) \in V_{ij}$, say $i = 1, \dots, N_1$, $j = 1, \dots, N_2$ in such a way that $\bar{\Omega} = \bigcup_{V_{ij} \in \mathcal{T}_h}$.

Further we denote σ_{ij}^{pq} with the 1D measure $m(\sigma_{ij}^{pq})$ the edges of finite volume V_{ij} and the distance between the neighbouring representative points we denote by $|x_{ij} - x_{i+p, j+q}| = d_{ij}^{pq}$, $|p| + |q| = 1$. Especially we denote $d_{1j}^{-10} = \text{dist}(x_{1j}, \partial\Omega)$ and $d_{N_1j}^{10} = \text{dist}(x_{N_1j}, \partial\Omega)$ due to Dirichlet boundary conditions. Unit outward normal vector to the edge σ_{ij}^{pq} we denote by \vec{n}_{ij}^{pq} , $|p| + |q| = 1$.

We denote the coefficient for the tensor and advection term for each finite volume V_{ij} and each edge σ_{ij}^{pq} in the form

$$B_{ij}^{pq} = \begin{pmatrix} b_{ij,pq}^{11} & b_{ij,pq}^{12} \\ b_{ij,pq}^{21} & b_{ij,pq}^{22} \end{pmatrix}, \quad (8)$$

$$\vec{A}_{ij}^{pq} = \begin{pmatrix} a_{ij,pq}^1 \\ a_{ij,pq}^2 \end{pmatrix}.$$

Remark. For our numerical approximation we can express all coefficients as a constant function on the whole edge for example by a value at the central point of an edge, which will be very useful for our purpose as we will see in the next section.

We propose here DDFV scheme as in Handlovičová (2016). This method was firstly used in Andreianov et al. (2007), and Domelevo and Omnes (2013).

In this case we have two meshes the first one is described above and the second one, we called it dual mesh is shifted to the north-east direction, consists of cells $\bar{V}_{ij} \in \bar{\mathcal{T}}_h$ with measure $m(\bar{V}_{ij})$ associated only with DF nodes \bar{x}_{ij} , say $i = 0, \dots, N_1$, $j = 0, \dots, N_2$ in such a way that \bar{x}_{ij} is the right top corner for the volume V_{ij} of the original mesh. Again, all inner dual finite volumes are rectangles and boundary volumes are created in such a way that $\bar{\Omega} = \bigcup_{\bar{V}_{ij} \in \bar{\mathcal{T}}_h}$.

All other entities are denote in similar way as for primal mesh but "barred".

We can define constant gradients on diamond cells as we can see in figure 1, which is the union

of \mathcal{D}_h and $\bar{\mathcal{D}}_h$, where

$$\mathcal{D}_h = \bigcup_{(i,j)=(0,0), \dots, (N_1, N_2)} D_{ij},$$

where D_{ij} has the vertices $\{x_{ij}, \bar{x}_{i,j-1}, x_{i+1,j}, \bar{x}_{ij}\}$ with degenerated (triangles) diamonds on the boundaries (for $i = 0$, or $i = N_1$) and

$$\bar{\mathcal{D}}_h = \bigcup_{(i,j)=(0,0), \dots, (N_1, N_2)} \bar{D}_{ij},$$

where \bar{D}_{ij} has the vertices $\{x_{ij}, \bar{x}_{ij}, x_{i,j+1}, \bar{x}_{i-1,j}\}$ with degenerated (triangles) diamonds on the boundaries (for $j = 0$, or $j = N_2$). Under this notation it is clear that $\bar{\Omega} = \mathcal{D}_h \cup \bar{\mathcal{D}}_h$ (see figure 1).

Then the gradient can be define for each time interval $[t_{n-1}, t_n]$ in the form:

$$\begin{aligned} \nabla u_{ij}^n &= \left(\frac{u_{i+1,j}^n - u_{ij}^n}{d_{ij}^{10}}, \frac{\bar{u}_{ij}^n - \bar{u}_{i,j-1}^n}{m(\sigma_{ij}^{10})} \right) = \\ &= (u_x^{ij,n}, u_y^{ij,n}) \text{ on } D_{ij}, \\ \nabla \bar{u}_{ij}^n &= \left(\frac{\bar{u}_{ij}^n - \bar{u}_{i-1,j}^n}{m(\sigma_{ij}^{01})}, \frac{u_{i,j+1}^n - u_{ij}^n}{d_{ij}^{01}} \right) = \\ &= (\bar{u}_x^{ij,n}, \bar{u}_y^{ij,n}) \text{ on } \bar{D}_{ij}. \end{aligned} \quad (9)$$

Following Handlovičová and Kotorová (2013) we have

Definition For time and space discretization described in this section we denote by (k, h) the time-space discretization of $(t_1, t_2) \times \Omega$. Then the function $u_{k,h}$ is in time and space piecewise constant function defined as follows:

$$u_{k,h}(x, y, \tau) = \frac{1}{2} \left(u_{k,h,V}(x, y, \tau) + u_{k,h,\bar{V}}(x, y, \tau) \right), \quad (10)$$

where

$$\begin{aligned} u_{k,h,V}(x, y, \tau) &= u_{ij}^n \text{ for } (x, y) \in V_{ij}, \\ \tau &\in ((n-1)k, nk] \\ u_{k,h,\bar{V}}(x, y, \tau) &= \bar{u}_{ij}^n \text{ for } (x, y) \in \bar{V}_{ij}, \\ \tau &\in ((n-1)k, nk]. \end{aligned}$$

Especially for every n -th time step we define

$$u_{n,h}(x, y) = \frac{1}{2} \left(u_{n,h,V}(x, y) + u_{n,h,\bar{V}}(x, y) \right), \quad (11)$$

where

$$\begin{aligned} u_{n,h,V}(x, y) &= u_{ij}^n \text{ for } (x, y) \in V_{ij}, \\ u_{n,h,\bar{V}}(x, y) &= \bar{u}_{ij}^n \text{ for } (x, y) \in \bar{V}_{ij} \end{aligned}$$



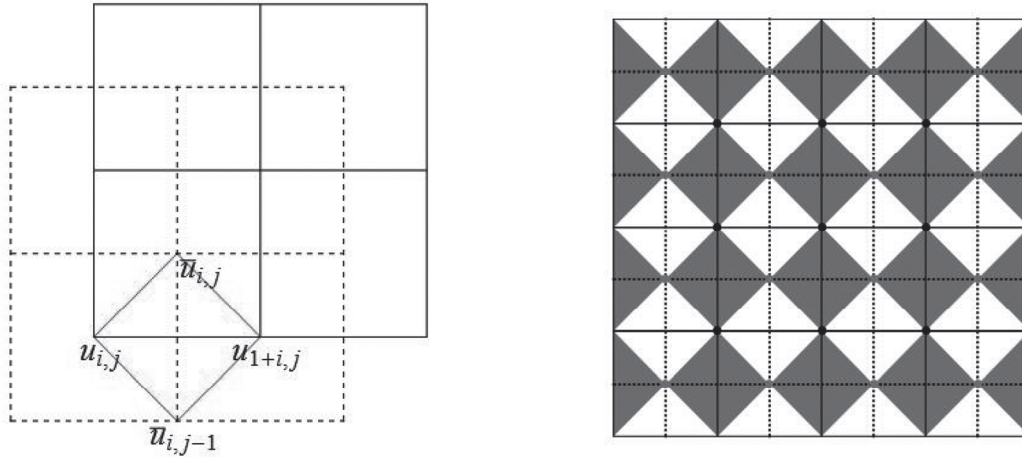


Fig. 1. Left: Diamond cell (red lines), where the gradient is constant, primal mesh (dashed lines), dual mesh (solid lines). Right: Diamonds D_{ij} (gray) and diamonds \bar{D}_{ij} (white) with primal-dual mesh and unknowns u (gray points) and \bar{u} (black points)

and

$$\delta u_{k,h}(x, y, \tau) = \frac{1}{2} \left(\delta u_{k,h,V}(x, y, \tau) + \delta u_{k,h,\bar{V}}(x, y, \tau) \right),$$

$$\delta u_{k,h,V}(x, y, \tau) = \frac{u_{ij}^n - u_{ij}^{n-1}}{k} \text{ for } (x, y) \in V_{ij}, \tau \in ((n-1)k, nk]$$

$$\delta u_{k,h,\bar{V}}(x, y, \tau) = \frac{\bar{u}_{ij}^n - \bar{u}_{ij}^{n-1}}{k} \text{ for } (x, y) \in \bar{V}_{ij}, \tau \in ((n-1)k, nk]. \tag{12}$$

and

$$\nabla u_{k,h}(x, y, \tau) = \begin{cases} \nabla u_{ij}^n & \text{for } (x, y) \in D_{ij}, \tau \in ((n-1)k, nk] \\ \nabla \bar{u}_{ij}^n & \text{for } (x, y) \in \bar{D}_{ij}, \tau \in ((n-1)k, nk] \end{cases} \tag{13}$$

Our computation domain is rectangle, so we can construct both meshes as super admissible mesh consisting of rectangles only with edges h_x in x-direction and h_y in y direction. In this case $m(V_{ij}) = m(\bar{V}_{ij}) = h_x h_y$, $m(\sigma_{ij}) = \bar{d}_{ij} = h_y$, $d_{ij} = m(\bar{\sigma}_{ij}) = h_x$. Our numerical method is derived in Handlovičová (2016). Here we present its final form.

For unknown value u_{ij}

$$\begin{aligned} & \frac{u_{ij}^n - u_{ij}^{n-1}}{k} h_x h_y + r u_{ij}^n h_x h_y - \\ & h_y [b_{ij,10}^{11} u_x^{ij,n} + b_{ij,10}^{12} u_y^{ij,n}] - \\ & h_x [b_{ij,01}^{21} \bar{u}_x^{ij,n} + b_{ij,01}^{22} \bar{u}_y^{ij,n}] + \\ & h_y [b_{ij,-10}^{11} u_x^{i-1j,n} + b_{ij,-10}^{12} u_y^{i-1j,n}] + h_x [b_{ij,0-1}^{21} \bar{u}_x^{i-1j,n} + b_{ij,0-1}^{22} \bar{u}_y^{i-1j,n}] + \\ & h_y a_{ij,10}^1 \frac{u_{i+1j}^n - u_{ij}^n}{2} + h_x a_{ij,01}^2 \frac{u_{ij+1}^n - u_{ij}^n}{2} - \\ & h_y a_{ij,-10}^1 \frac{u_{i-1j}^n - u_{ij}^n}{2} - h_x a_{ij,0-1}^2 \frac{u_{ij-1}^n - u_{ij}^n}{2} \\ & = f_{ij}^n h_x h_y. \end{aligned} \tag{14}$$

For unknown value \bar{u}_{ij} we have

$$\begin{aligned} & \frac{\bar{u}_{ij}^n - \bar{u}_{ij}^{n-1}}{k} h_x h_y + r \bar{u}_{ij}^n h_x h_y - \\ & h_y [b_{i+1j+1,0-1}^{11} \bar{u}_x^{i+1,j} + b_{i+1j+1,0-1}^{12} \bar{u}_y^{i+1,j}] - \\ & h_x [b_{i+1j+1,-10}^{21} u_x^{i,j+1} + b_{i+1j+1,-10}^{22} u_y^{i,j+1}] + \\ & h_y [b_{ij,01}^{11} \bar{u}_x^{i,j} + b_{ij,01}^{12} \bar{u}_y^{i,j}] + \\ & h_x [b_{ij,11}^{21} u_x^{i,j} + b_{ij,10}^{22} u_y^{i,j}] + \\ & h_y a_{i+1j+1,0-1}^1 \frac{\bar{u}_{i+1j}^n - \bar{u}_{i,j}^n}{2} - \\ & h_x a_{i+1j+1,-10}^2 \frac{\bar{u}_{ij+1}^n - \bar{u}_{i,j}^n}{2} - \\ & h_y a_{ij,01}^1 \frac{\bar{u}_{i-1j}^n - \bar{u}_{i,j}^n}{2} - \\ & h_x a_{ij,10}^2 \frac{\bar{u}_{ij-1}^n - \bar{u}_{i,j}^n}{2} = \bar{f}_{ij}^n h_x h_y. \end{aligned} \tag{15}$$



4. STABILITY ESTIMATES

For further considerations we must use the properties of our data, that means the coefficients of matrix \mathbf{B} and advection vector \vec{A} and a special construction of our primal and dual mesh. Moreover we use $a_{ij}^1 = \frac{1}{2}y_{ij} + \frac{1}{2}\rho\sigma - r$ and $a_{ij}^2 = \frac{1}{2}\sigma^2 - \kappa\theta + \kappa y_{ij}$.

Theorem 1. *Let the discretization mesh has the properties described in section 2 and k , h_x , h_y have the same meaning and let there exists constant C_h such that it hold $h_y = C_h h_x$. Let the Fichera condition (4) be fulfilled and let it holds*

$$\sigma \geq \rho, \quad 1 \geq \rho\sigma. \quad (16)$$

$$Y(\lambda + \kappa) \geq \kappa\theta - \frac{1}{2}\sigma^2. \quad (17)$$

Then for our numerical solution the following stability estimates holds:

$$\|u_{k,h}\|_{L_\infty(I;L_2(\Omega))} \leq C \quad (18)$$

where C is generic constant depending only on data of the problem and not on parameters k , h_x , h_y .

Proof. We notice that h_y is the size of vertical diagonal of each D_{ij} and h_x the size of horizontal diagonal of D_{ij} . We denote by b_{ij} , a_{ij} the coefficients of the tensor and convection terms from the equation evaluated at the barycentre of D_{ij} . Analogously h_x is the size horizontal diagonal of \bar{D}_{ij} , h_y the size of vertical diagonal of \bar{D}_{ij} and \bar{b}_{ij} , \bar{a}_{ij} the coefficients of the tensor and convection terms from the equation evaluated at the barycentre of \bar{D}_{ij} .

First we multiply all equations (14) by ku_{ij}^n and sum over all finite volumes of the primal mesh. Using the usual finite volume property and the fact that the solution fulfils zero Dirichlet and Neumann boundary condition with Fichera condition on the bottom side

we have

$$\begin{aligned} & (1 + 2kr) \sum_{V_{ij} \in \mathcal{T}} (u_{ij}^n)^2 h_x h_y + \\ & \sum_{V_{ij} \in \mathcal{T}} (u_{ij}^n - u_{ij}^{n-1})^2 h_x h_y + \\ & 2k \sum_{D_{ij} \in \mathcal{D}_h} \left(h_x h_y \left(b_{ij}^{11} (u_x^{ij,n})^2 + b_{ij}^{12} u_y^{ij,n} u_x^{ij,n} \right) + \right. \\ & \left. h_y \frac{a_{ij}^1}{2} ((u_{i+1j}^n)^2 - (u_{ij}^n)^2) \right) + \\ & 2k \sum_{\bar{D}_{ij} \in \bar{\mathcal{D}}_h} \left(h_x h_y \left(\bar{b}_{ij}^{22} (\bar{u}_y^{ij,n})^2 + \bar{b}_{ij}^{21} \bar{u}_x^{ij,n} \bar{u}_y^{ij,n} \right) + \right. \\ & \left. h_x \frac{\bar{a}_{ij}^2}{2} ((\bar{u}_{ij+1}^n)^2 - (\bar{u}_{ij}^n)^2) \right) = \\ & \sum_{V_{ij} \in \mathcal{T}} (u_{ij}^{n-1})^2 h_x h_y + 2k \sum_{V_{ij} \in \mathcal{T}} f_{ij}^n u_{ij}^n h_x h_y \end{aligned} \quad (19)$$

and analogously for the unknowns of the dual mesh:

$$\begin{aligned} & (1 + 2kr) \sum_{\bar{V}_{ij} \in \bar{\mathcal{T}}} (\bar{u}_{ij}^n)^2 h_x h_y + \\ & \sum_{\bar{V}_{ij} \in \bar{\mathcal{T}}} (\bar{u}_{ij}^n - \bar{u}_{ij}^{n-1})^2 h_x h_y + \\ & 2k \sum_{D_{ij} \in \mathcal{D}_{h,int}} \left(h_x h_y \left(b_{ij}^{22} (u_y^{ij,n})^2 + b_{ij}^{12} u_y^{ij,n} u_x^{ij,n} \right) + \right. \\ & \left. h_y \frac{a_{ij}^2}{2} ((\bar{u}_{ij}^n)^2 - (\bar{u}_{ij-1}^n)^2) \right) + \\ & 2k \sum_{\bar{D}_{ij} \in \bar{\mathcal{D}}_{h,int}} \left(h_x h_y \left(\bar{b}_{ij}^{11} (\bar{u}_x^{ij,n})^2 + \right. \right. \\ & \left. \left. \bar{b}_{ij}^{21} \bar{u}_x^{ij,n} \bar{u}_y^{ij,n} \right) + h_x \frac{\bar{a}_{ij}^1}{2} ((\bar{u}_{ij}^n)^2 - (\bar{u}_{i-1j}^n)^2) \right) = \\ & \sum_{\bar{V}_{ij} \in \bar{\mathcal{T}}} (\bar{u}_{ij}^{n-1})^2 h_x h_y + 2k \sum_{\bar{V}_{ij} \in \bar{\mathcal{T}}} \bar{f}_{ij}^n \bar{u}_{ij}^n h_x h_y. \end{aligned} \quad (20)$$

Putting both equations (19), (20) together we obtain



Now summing for $n = 1, \dots, m$ we have

$$\begin{aligned}
 & \sum_{V_{ij} \in \mathcal{T}} (u_{ij}^m)^2 h_x h_y + \sum_{\bar{V}_{ij} \in \bar{\mathcal{T}}} (\bar{u}_{ij}^m)^2 h_x h_y + \\
 & + 2kr \sum_{n=1}^m \left(\sum_{V_{ij} \in \mathcal{T}} (u_{ij}^n)^2 h_x h_y + \sum_{\bar{V}_{ij} \in \bar{\mathcal{T}}} (\bar{u}_{ij}^n)^2 h_x h_y \right) + \\
 & \sum_{n=1}^m \left(\sum_{V_{ij} \in \mathcal{T}} (u_{ij}^n - u_{ij}^{n-1})^2 h_x h_y + \sum_{\bar{V}_{ij} \in \bar{\mathcal{T}}} (\bar{u}_{ij}^n - \bar{u}_{ij}^{n-1})^2 h_x h_y \right) + \\
 & (1 + 2kr) \left(\sum_{V_{ij} \in \mathcal{T}} (u_{ij}^n)^2 h_x h_y + \sum_{\bar{V}_{ij} \in \bar{\mathcal{T}}} (\bar{u}_{ij}^n)^2 h_x h_y \right) + \\
 & \left(\sum_{V_{ij} \in \mathcal{T}} (u_{ij}^n - u_{ij}^{n-1})^2 h_x h_y + \sum_{\bar{V}_{ij} \in \bar{\mathcal{T}}} (\bar{u}_{ij}^n - \bar{u}_{ij}^{n-1})^2 h_x h_y \right) + \\
 & 2k \sum_{D_{ij} \in \mathcal{D}_h} \left(b_{ij}^{11} (u_x^{ij,n})^2 + b_{ij}^{22} (u_y^{ij,n})^2 + 2b_{ij}^{12} u_y^{ij,n} u_x^{ij,n} \right) h_x h_y + \\
 & 2k \sum_{\bar{D}_{ij} \in \bar{\mathcal{D}}_h} \left(\bar{b}_{ij}^{22} (\bar{u}_y^{ij,n})^2 + \bar{b}_{ij}^{11} (\bar{u}_x^{ij,n})^2 + 2\bar{b}_{ij}^{21} \bar{u}_x^{ij,n} \bar{u}_y^{ij,n} \right) h_x h_y + A_1 + A_2 = \\
 & 2k \sum_{D_{ij} \in \mathcal{D}_h} \left(b_{ij}^{11} (u_x^{ij,n})^2 + b_{ij}^{22} (u_y^{ij,n})^2 + 2b_{ij}^{12} u_y^{ij,n} u_x^{ij,n} \right) h_x h_y + \\
 & 2k \sum_{\bar{D}_{ij} \in \bar{\mathcal{D}}_h} \left(\bar{b}_{ij}^{22} (\bar{u}_y^{ij,n})^2 + \bar{b}_{ij}^{11} (\bar{u}_x^{ij,n})^2 + 2\bar{b}_{ij}^{21} \bar{u}_x^{ij,n} \bar{u}_y^{ij,n} \right) h_x h_y + \\
 & 2kh_y \sum_{D_{ij} \in \mathcal{D}_h} \left(\frac{a_{ij}^1}{2} ((u_{i+1,j}^n)^2 - (u_{ij}^n)^2) + \frac{a_{ij}^2}{2} ((\bar{u}_{ij}^n)^2 - (\bar{u}_{ij-1}^n)^2) \right) + \\
 & 2kh_x \sum_{\bar{D}_{ij} \in \bar{\mathcal{D}}_h} \left(\frac{\bar{a}_{ij}^2}{2} ((u_{ij+1}^n)^2 - (u_{ij}^n)^2) + \frac{\bar{a}_{ij}^1}{2} ((\bar{u}_{ij}^n)^2 - (\bar{u}_{i-1,j}^n)^2) \right) = \\
 & \sum_{V_{ij} \in \mathcal{T}} (u_{ij}^{n-1})^2 h_x h_y + \sum_{\bar{V}_{ij} \in \bar{\mathcal{T}}} (\bar{u}_{ij}^{n-1})^2 h_x h_y + \\
 & 2k \sum_{V_{ij} \in \mathcal{T}} f_{ij}^n u_{ij}^n h_x h_y + 2k \sum_{\bar{V}_{ij} \in \bar{\mathcal{T}}} \bar{f}_{ij}^n \bar{u}_{ij}^n h_x h_y. \tag{21}
 \end{aligned}$$

where

$$\begin{aligned}
 A_1 &= 2kh_y \sum_{n=1}^m \sum_{D_{ij} \in \mathcal{D}_h} \left(\frac{a_{ij}^1}{2} ((u_{i+1,j}^n)^2 - (u_{ij}^n)^2) + \frac{a_{ij}^2}{2} ((\bar{u}_{ij}^n)^2 - (\bar{u}_{ij-1}^n)^2) \right), \\
 A_2 &= 2kh_x \sum_{n=1}^m \sum_{\bar{D}_{ij} \in \bar{\mathcal{D}}_h} \left(\frac{\bar{a}_{ij}^2}{2} ((u_{ij+1}^n)^2 - (u_{ij}^n)^2) + \frac{\bar{a}_{ij}^1}{2} ((\bar{u}_{ij}^n)^2 - (\bar{u}_{i-1,j}^n)^2) \right)
 \end{aligned}$$

Now we estimate the term A_1 . For the first part of this term we can see that it vanishes due to the form of the terms a_{ij}^1 and Dirichlet boundary conditions on the vertical parts of the boundary. For the second term of this expression notice the form of the coefficients a_{ij}^2 .



We can write:

$$\begin{aligned}
 A_1 = & kh_y \left(\frac{1}{2} \sigma^2 - \kappa \theta \right) \sum_{n=1}^m \sum_{i=1}^{N1} \left((\overline{u}_{i,N2}^n)^2 - (\overline{u}_{i0}^n)^2 \right) - \\
 & - kh_y^2 (\lambda + \kappa) \sum_{n=1}^m \sum_{\overline{V}_{ij} \in \overline{\mathcal{T}}} (\overline{u}_{ij}^n)^2 + \\
 & + kh_y^2 (\lambda + \kappa) (N2 - 1) \sum_{i=1}^{N1} (\overline{u}_{i,N2}^n)^2.
 \end{aligned} \quad (23)$$

Analogously we obtain

$$\begin{aligned}
 A_2 = & 2kh_x \left(\frac{1}{2} \sigma^2 - \kappa \theta \right) \sum_{n=1}^m \sum_{i=1}^{N1} \left((u_{i,N2}^n)^2 - (u_{i0}^n)^2 \right) - \\
 & - kh_x h_y (\lambda + \kappa) \sum_{n=1}^m \sum_{V_{ij} \in \mathcal{T}} (u_{ij}^n)^2 + \\
 & + kh_x h_y N2 (\lambda + \kappa) \sum_{i=1}^{N1} (u_{i,N2}^n)^2.
 \end{aligned} \quad (24)$$

Following Handlovičová (2016) we can estimate for all finite volumes

$$\begin{aligned}
 2b_{ij}^{12} u_y^{ij,n} u_x^{ij,n} & \leq |b_{ij}^{12}| (u_x^{ij,n})^2 + |b_{ij}^{12}| (u_y^{ij,n})^2, \\
 2\overline{b}_{ij}^{21} \overline{u}_x^{ij,n} \overline{u}_y^{ij,n} & \leq |\overline{b}_{ij}^{21}| (\overline{u}_x^{ij,n})^2 + |\overline{b}_{ij}^{21}| (\overline{u}_y^{ij,n})^2.
 \end{aligned} \quad (25)$$

Now we can use the assumptions (16) of the theorem. We have (the same for "overlined" coefficients)

$$b_{ij}^{11} - |b_{ij}^{12}| = \frac{y_{ij}}{2} (1 - \rho\sigma) > 0$$

$$b_{ij}^{22} - |b_{ij}^{12}| = \frac{y_{ij}}{2} (\sigma^2 - \rho\sigma) > 0.$$

Now we denote

$$c = \min\{(1 - \rho\sigma, \sigma^2 - \rho\sigma)\}.$$

Take all these estimation together and due to zero

initial boundary condition we can write

$$\begin{aligned}
 & \sum_{V_{ij} \in \mathcal{T}} (u_{ij}^m)^2 h_x h_y + \sum_{\overline{V}_{ij} \in \overline{\mathcal{T}}} (\overline{u}_{ij}^m)^2 h_x h_y + \\
 2kr & \sum_{n=1}^m \left(\sum_{V_{ij} \in \mathcal{T}} (u_{ij}^n)^2 h_x h_y + \sum_{\overline{V}_{ij} \in \overline{\mathcal{T}}} (\overline{u}_{ij}^n)^2 h_x h_y \right) + \\
 & kc \sum_{n=1}^m \sum_{D_{ij} \in \mathcal{D}_h} y_{ij} \nabla u_{ij}^n h_x h_y + \\
 & k \sum_{n=1}^m \sum_{\overline{D}_{ij} \in \overline{\mathcal{D}}_h} \overline{y}_{ij} \nabla \overline{u}_{ij}^n h_x h_y + A_1 + A_2 \leq \\
 2\|f_{k,h}\|_{L_2(I, L_2(\Omega))}^2 & + 2k \sum_{n=1}^m \sum_{V_{ij} \in \mathcal{T}} (u_{ij}^n)^2 h_x h_y + \\
 & 2k \sum_{n=1}^m \sum_{\overline{V}_{ij} \in \overline{\mathcal{T}}} (\overline{u}_{ij}^n)^2 h_x h_y.
 \end{aligned} \quad (26)$$

If (17) holds then

$$\begin{aligned}
 A_1 + A_2 & \geq -kh_y^2 (\lambda + \kappa) \sum_{n=1}^m \sum_{\overline{V}_{ij} \in \overline{\mathcal{T}}} (\overline{u}_{ij}^n)^2 - \\
 & kh_x h_y (\lambda + \kappa) \sum_{n=1}^m \sum_{V_{ij} \in \mathcal{T}} (u_{ij}^n)^2 + \\
 kh_y & \left(Y(\lambda + \kappa) + \frac{1}{2} \sigma^2 - \kappa \theta \right) \sum_{i=1}^{N1} (\overline{u}_{i,N2}^n)^2 + \\
 kh_x & \left(Y(\lambda + \kappa) + \frac{1}{2} \sigma^2 - \kappa \theta \right) \sum_{i=1}^{N1} (u_{i,N2}^n)^2.
 \end{aligned} \quad (27)$$

Finally we have

$$\begin{aligned}
 & \sum_{V_{ij} \in \mathcal{T}} (u_{ij}^m)^2 h_x h_y + \sum_{\overline{V}_{ij} \in \overline{\mathcal{T}}} (\overline{u}_{ij}^m)^2 h_x h_y + \\
 2kr & \sum_{n=1}^m \left(\sum_{V_{ij} \in \mathcal{T}} (u_{ij}^n)^2 h_x h_y + \sum_{\overline{V}_{ij} \in \overline{\mathcal{T}}} (\overline{u}_{ij}^n)^2 h_x h_y \right) + \\
 & kc \sum_{n=1}^m \sum_{D_{ij} \in \mathcal{D}_h} y_{ij} \nabla u_{ij}^n h_x h_y + \\
 & k \sum_{n=1}^m \sum_{\overline{D}_{ij} \in \overline{\mathcal{D}}_h} \overline{y}_{ij} \nabla \overline{u}_{ij}^n h_x h_y \leq \\
 & 2\|f_{k,h}\|_{L_2(I, L_2(\Omega))}^2 + \\
 k & \left(2 + \max\{1, C_h\} (\lambda + \kappa) \right) \sum_{n=1}^m \left(\sum_{V_{ij} \in \mathcal{T}} (u_{ij}^n)^2 h_x h_y + \right. \\
 & \left. \sum_{\overline{V}_{ij} \in \overline{\mathcal{T}}} (\overline{u}_{ij}^n)^2 h_x h_y \right).
 \end{aligned} \quad (28)$$



Thus using the properties of function $f(x, t)$ and Gronwall lemma we can conclude

$$\|u_{m,h}\|_{L_2(\Omega)}^2 + 2r\|u_{k,h}\|_{L_2(I,L_2(\Omega))}^2 + 2ch_y\|\nabla u_{k,h}\|_{L_2(I,L_2(\Omega))}^2 \leq C \quad (29)$$

for arbitrary $m = 1, \dots, N$ which conclude the proof.

Now if we follow the idea of Olejnik and Radkevich (1971), we can regularize our equation (6) and the numerical scheme as well with ε Laplacian term so we obtain regularized problem

$$\frac{\partial u}{\partial \tau} + \vec{A} \cdot \nabla u = \varepsilon \Delta u + \nabla \cdot (\mathbf{B} \nabla u) - ru + f(x, y, \tau), \text{ in } \Omega \times [t_1, t_2], \quad (30)$$

and similarly we regularize numerical scheme. In this case we straightforward can obtain

Theorem 2. *Let the assumptions of theorem 1. hold and let $\varepsilon > 0$ be fixed regularization parameter as in problem (30). Then for our regularized numerical solution (we denote it by $u_{k,h,\varepsilon}$ the following stability estimates holds:*

$$\|u_{k,h,\varepsilon}\|_{L_\infty(I;L_2(\Omega))} + \|\nabla u_{k,h,\varepsilon}\|_{L_2(I,L_2(\Omega))} \leq C(\varepsilon) \quad (31)$$

where $C(\varepsilon)$ is generic constant depending only on regularized parameter ε and other data of the problem and not on parameters k, h_x, h_y .

5. NUMERICAL EXPERIMENTS

In this section we want to present two examples where the influence of regularization parameter ε in the model 30 is shown.

Experiment - Heston model

Numerical experiment for Heston model using DDFV method and its comparing with the classical FV method can be found in Handlovičová (2016).

Here we focused on comparing DDFV scheme with the scheme for regularized problem (30).

The data of the experiment have the following values: $\rho = -0.5, \sigma = 0.5, r = 0.1, \kappa = 5., \theta = 0.07, \lambda = 0, E = 100$.

Computational domain is of the form:

$$\Omega = \{(x, y) \in \mathbb{R}^2 \mid -7 \leq x \leq 3, 0 \leq y \leq 1\}.$$

We compute the problem on the time interval $[0, 0.05]$

and the initial and boundary conditions are :

$$\begin{aligned} u(x, y, 0) &= \max(0, e^x - 1), \\ u(-7, y, \tau) &= 0, \quad u(3, y, \tau) = e^3 - e^{-r\tau}, \\ \frac{\partial u}{\partial y}(x, 0, \tau) &= 0, \quad \frac{\partial u}{\partial y}(x, 1, \tau) = 0. \end{aligned}$$

For comparing results obtained by proposed method and the method used in Kútík (2013) we use the same definition of L_2 error. That means we compute the error only on the sub domain $\langle -1, 1 \rangle \times \langle 0, 1 \rangle$. When we take into account the used transformation $x = \ln \frac{S}{E}$ in Heston model we obtain for variable S which represent price of the underlying asset the interval $\langle 36, 272 \rangle$ which represent the usual interval for underlying asset prices. For more detail see Kútík (2013). Results are presented in the table 1, where N_x, N_y is number of finite volumes of primal mesh along the horizontal boundary respectively vertical boundary. N_{ts} is number of computed time steps. We denote by L_2D the errors for DDFV scheme and by L_2R the errors for regularized DDFV scheme where $\varepsilon = 0.0001$. As one can see in table 1. the results for sufficiently small ε are almost the same as for the non regularized case.

Experiment - Diffusion model

In this experiment we want to compare the results obtained for nonregularized model with the regularized one. For this purpose we use the experiment from Kútík (2013) for tensor diffusion only, where the exact solution is known and is everywhere positive. We compare the results obtained DDFV method with original problem with the regularized model. For this example the model is of the form

$$\frac{\partial u}{\partial \tau} = \nabla \cdot (\mathbf{B} \nabla u).$$

with Dirichlet boundary and initial conditions arises from the exact solution

$$u(\mathbf{x}, \tau) = \frac{1}{4\pi\tau\sqrt{|\mathbf{B}|}} e^{-\frac{\mathbf{x}^T \mathbf{B}^{-1} \mathbf{x}}{4\tau}},$$

$$\mathbf{x} \in \Omega \subset \mathbb{R}^2, \tau \in \langle t_1, t_2 \rangle, t_1, t_2 \in \mathbb{R}, t_2 > t_1 > 0.$$

where $|\mathbf{B}|$ represents determinant and \mathbf{B}^{-1} is inverse matrix of positive-definite diffusion tensor \mathbf{B} .

The results can be compared with those obtained by classical finite volume method presented in Kútík (2013) and they can be seen in table 2. As one can observe on figures 2 both numerical solutions have problem with negative regions although the exact solution is positive. We can see negative stripes in profiles of numerical solutions, although they are better



Table 1. Results for Heston model, regularized DDFV scheme (R) and DDFV scheme (D)

N_x	N_y	N_{ts}	k	L_2R	L_2D
20	10	1	0.05	0.00318475	0.00318557
40	20	4	0.0125	0.00206035	0.00206132
80	40	16	0.003125	0.00151170	0.00151241
160	80	64	0.000781	0.00124956	0.00125001

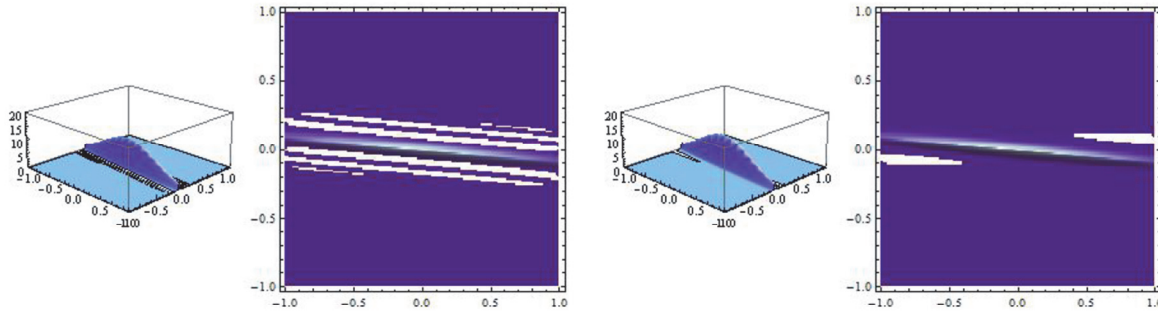
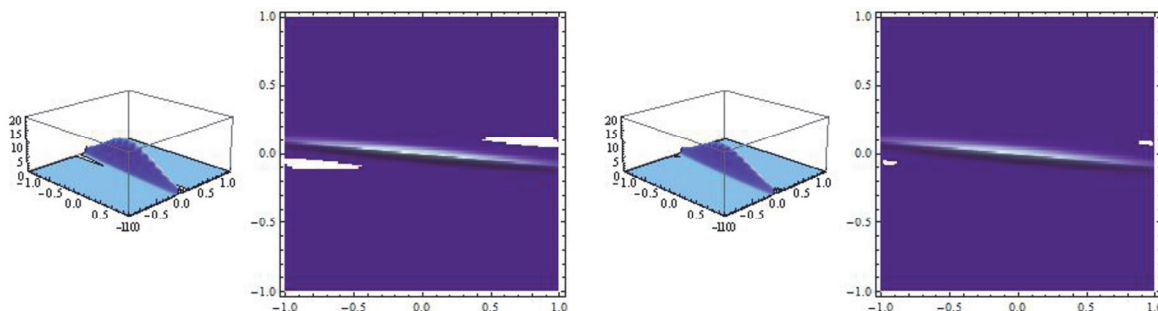

Fig. 2. Left: Results using classical FV method $N_x = 160$, numerical solution and negative stripes of the numerical solution. Right: Results using discrete dual FV method $N_x = 160$, numerical solution and negative stripes of the numerical solution.

Table 2. Results obtained for classical finite volume method (C) and for DDFV method (D)

$N_x = N_y$	N_{ts}	$h_x = h_y$	k	L_2C	L_2D	EOC_C	EOC_D
20	10	0.1	0.01	0.2027	0.1348		
40	40	0.05	0.0025	0.1919	0.0549	0.0788	1.2944
80	160	0.025	0.000625	0.1133	0.0214	0.7612	1.3631
160	640	0.0125	0.000156	0.0474	0.0070	1.2579	1.6059

Table 3. Results obtained for classical finite volume method (C) and for DDFV method (D)

$N_x = N_y$	N_{ts}	$h_x = h_y$	k	L_2C	L_2D	EOC_C	EOC_D
20	10	0.1	0.01	0.1349	0.1370		
40	40	0.05	0.0025	0.0539	0.0587	1.32416	1.2248
80	160	0.025	0.000625	0.0174	0.05740	1.63104	0.0328
160	640	0.0125	0.000156	0.00601	0.0717	1.5329	-0.320


Fig. 3. Left: Results using regularized DDFV method $N_x = 160$, $\varepsilon = 0.00012$, numerical solution and negative stripes of the numerical solution. Right: Results using regularized DDFV method $N_x = 160$, $\varepsilon = 0.0012$, numerical solution and negative stripes of the numerical solution.


for DDVF scheme but on the contrary there are two times more computed points.

Regularized model was computed for regularization parameters $\varepsilon = 0.00012$ (we denote it by L_21 and EOC_1) and for regularization parameters $\varepsilon = 0.0012$ (we denote it by L_22 and EOC_2). The results can be found in table 3. As one can see from table 3, and figures 3 the regularization parameter can improve the problem with negative stripes for the numerical solution, but where the value of regularization parameter is "large" the stripes can be almost vanish but the solution is smaller everywhere, which gives worse L_2 errors.

6. CONCLUSIONS

We presented discrete duality finite volume scheme for Heston model. Main stability result is proved in theorem 1. where the $L_\infty([t_1, t_2], L_2(\Omega))$ estimate for the numerical solution is presented. For regularized model (30) estimates for the gradient of a numerical solution can be obtained. Numerical experiments using proposed method for Heston model and comparing it with previous numerical scheme are included in the section 4. The experiment for the diffusion model where we present also the experiments with regularized model conclude the section 4. Numerical experiments confirm the efficiency of presented scheme so the convergence of the numerical solution is worth proving for the future work.

REFERENCES

- Andreianov B., Boyer F., Hubert F., 2007, Discrete duality finite volume schemes for Leray-Lions-type elliptic problems on general 2D meshes, *Numer. Methods Partial Differential Equations*, 2, 1, 145-195.
- Black F., Scholes M., 1973, The pricing of options and corporate liabilities, *The Journal of Political Economy*, 81, 3, 637-654.
- Domelevo K., Omnes P., 2013, A finite volume method for the Laplace equation on almost arbitrary two-dimensional grids, *M2AN*, 39, 6, 1203-124.
- Handlovičová A., 2016, Discrete duality finite volume scheme for solving Heston model, *Proceedings of ALGORITMY*, 264-274.
- Handlovičová A., Kotorová D., 2013, Convergence of a semi-implicit discrete duality finite volume scheme for the curvature driven level set equation in 2D, *Kybernetika*, 49, 6, 829-854.
- Heston S.L., 1993, A Closed-Form Solution for Options with Stochastic Volatility with Applications to Bond and Currency Options. *The Review of Financial Studies*, 6, 2, 327-343.
- Kútik P., 2013, Numerical solution of partial differential equations in financial mathematics, *Dissertation Thesis*, Bratislava.

Kútik P., Mikula K., 2015, Diamond-cell finite volume scheme for the Heston model, *Discrete and Continuous Dynamical Systems - Series S (DCDS-S)*, 8, 913-931.

Olejník O.A., Radkevich E.V., 1971, Second order equations with non-negative characteristic form, *VINITI Acad. Nauk SSSR*, Moscow.

OSZACOWANIE STABILNOŚCI SCHEMATU DYSKRETNIE DUALNYCH OBJĘTOŚCI SKOŃCZONYCH DLA MODELU HESTONA

Streszczenie

Tensorowe równanie dyfuzji jest ważnym modelem w wielu obszarach nauki. W pracy skupiono się na problemie, który występuje w matematyce finansowej i jest znany jako dwuwymiarowy model Hestona. Zaprezentowano oszacowanie stabilności dla dyskretnego, dualnego schematu objętości skończonych. W pracy zamieszczono wyniki numerycznych eksperymentów przeprowadzonych z wykorzystaniem zaproponowanej metody, które porównano z opublikowanymi wcześniej schematami numerycznymi.

Received: December 19, 2016

Received in a revised form: April 6, 2017

Accepted: April 12, 2017

